Design and Analysis of a New Type Integrated Magnetic-geared Motor for Oil Pumping Units

Zhongxue Yang [a], Yubo Duan [b]

School of Electrical Engineering & Information, Northeast Petroleum University, Daqing 163000, China

[a]yzx@hrbust.edu.cn, [b]eienepu@163.com

Abstract

This paper presents an integrated magnetic-geared motor used in the oil pumping units. The new motor combines lots of the advantages of the traditional permanent magnet motor and permanent magnet gear, and the compact motor will take a place in industrial production with the advantages of high output torque density and no need of the deceleration device, therefore, the research and development of the magnetic-geared integrated motor have practical significance both for the theoretical research or production. For the proposed integrated motor, the proportion of pole-pieces and the pole arc angle are analyzed and discussed. The static and dynamic performances of the motor are calculated using the 2-D finite element method (FEM), which verifies the effectiveness of the theoretical analysis.

Keywords

High Torque Density, Finite Element Method, Oil Pumpig Units, Flux Modulation.

1. Introduction

With the development of industrial technology, low speed and high torque direct drive is more and more competitive for industrial production, for example, electric vehicles and the oil pumping units. In order to obtain the characteristic of low-speed large-torque output in the industrial production, the motor and gear reduction mechanism are generally used together, it will not only increase the size and weight of the entire system greatly, but also accompanied by the problem of noise and efficiency reduction, so the low-speed direct-drive motors with low noise, high torque density and reliable operation are needed in the industry. In the past two years, the new inventions, new technologies and new structures have been coming out one after the other in the field of new energy applications. The new type of concentric magnetic gears has provided a new way for the development of high torque density motors. Magnetic-geared-integrated motor is the new motor which combined the permanent magnet gear topology and conventional permanent magnet motor based on the principle of magnetic field modulation.

In 2001, the magnetic gear is presented by professor D. Howe at the University of Sheffield in UK [1] and it attracts increasing attention because of its the advantages of high reliability, low noise, maintenance-free, physical isolation and inherent overload protection, and some magnetic gears structure were proposed due to the competitive torque transmission capability and efficiency compared with mechanical gears [2-3]. A novel flux-controllable vernier permanent-magnet motor [4] is proposed to provide low speed operation with high torque output, and the DC field winding and the vernier structure were integrated artfully together, and the same vernier machine with outer-rotor permanent magnet was proposed for wind power generation[5]. Parallel hybrid excitation flux-switch machines that consist of permanent magnet and field excitation coil as their main flux sources have several attractive features such as high power factor compared to electrically excited synchronous motors, smaller armature reaction reactance, and the air-gap magnetic field that can be adjusted flexibly compared to PM synchronous motors [6]. Based on the space-vector pulse width modulation and wide-speed sliding mode observer, a new flux-modulated permanent-magnet wheel motor [7] was presented, and it has the advantages of low torque/flux ripple. In reference [8], A new field

controlled axial flux surface mounted permanent magnet machine has been proposed not only overcome the drawback of PM motor but also to improve the features by introducing a new axial flux structure with flux weakening capability. Some methods are proposed to reduce the torque ripples based on the radial magnetic-field-modulated brushless double-rotor machine in reference [9].

In this paper, a prototype was designed for oil pumping units, and the purpose of it is to integrated magnetic-gear into PM so that the high torque and low-speed requirement for direct driving can be achieved simultaneously. First of all, the characteristics of magnetic field modulation permanent magnetic gear was introduced and its magnetic field modulation principle through the analytic method was deduced to establish the mathematical model. Secondly, according to the requirements of different working conditions, the best solution is chosen, and the original motor structure is optimized. Finally, the new concept of magnetic-geared-integrated machine was calculated and analyzed based on the 2-D FEM, and the calculation results show the validity of the motor design.

2. Proposed Machine and Operation Principle

2.1 Machine Topology.

A designed integrated magnetic-geared motor is shown in Fig.1, and in order to observe the specific structure clearly, the three-dimensional structure modeling of the novel integrated motor is shown in Fig.2.

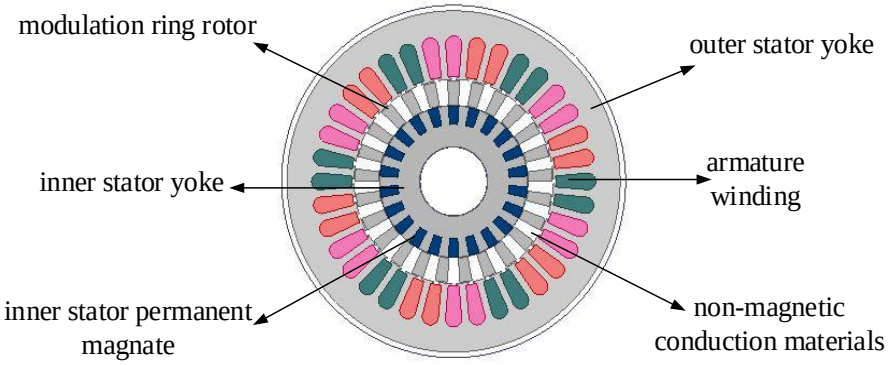

Fig.1 Cross section of the designed motor.

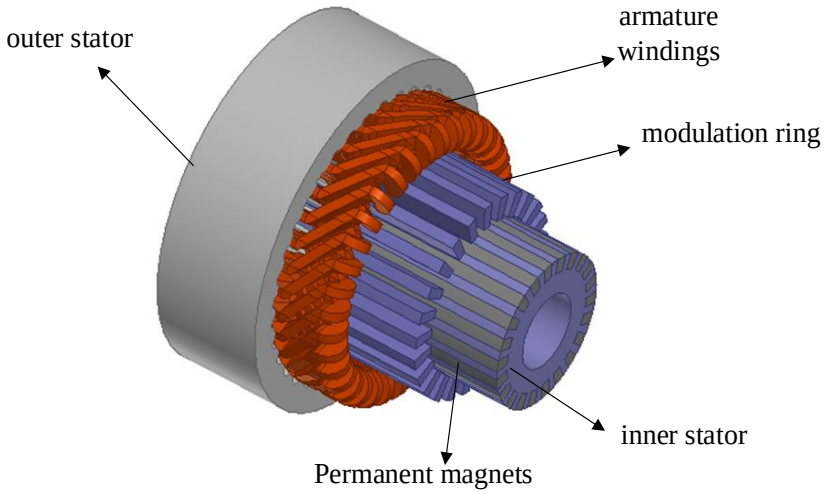

Fig.2 The 3D structure of the new magnetic field modulated motor

The motor has dual stator and double air gap, in addition, the modulation ring is used as rotor. There are 36 slots in the outer stator occupied by single-layer and three-phase concentrated windings, besides, all PMs are magnetized in the same direction and embedded in the inner stator. The modulation ring consists of magnetic conduction pieces and non-magnetic conduction materials that can provide a reliable fixation effect, and these two parts are alternately distributed along the

circumference. Non-magnetic conduction parts can be filled with non-magnetic material, such as epoxy resin casting, to increase the modulation ring strength. As can be seen from the structural diagram, the rotating part of the motor is optional, that is, the modulation ring can be used as a rotor, or the inner stator can be arranged as a rotor. In the process of simulation, the motor will be researched in different operating situations . In addition, the C type permanent magnet structure was adopted in this paper, which can reduce effectively the amount of material and the motor volume, so the power density of the motor can be improved.

2.2 Operation Principle.

The novel integrated magnetic-geared motor operates on the flux modulation principle due to modulation ring. The output speed of modulation ring, in the middle of the integrated magnetic-geared motor, is determined by the supply frequency and pole pairs, and the specific relationship is shown as the following formula.

$$N_s = P_i + P_o \tag{1}$$

$$G_r = -\frac{P_o}{P_i} \tag{2}$$

$$\Omega_o = G_r \frac{60f}{P_i} = -\frac{60f}{P_o} \tag{3}$$

Where P_i is the number of rotating poles formed by the three-phase current, N_s is the number of magnetic conduction pieces of the modulation ring, f is the power frequency, P_o is the pole pairs of the inner stator, G_r is the speed ratio, and Ω_o is the mechanical speed of the modulation ring.The parameters of designed motor are shown in Table 1. The rated speed is 600rpm, the frequency is 250Hz, the stator winding resistance per phase is 0.19Ω.

Table 1. specification of proposed machine

Structure of rotor	Modulation ring rotor
Rotor and stator core material	D23-50
Outer stator outside radius (mm)	184
Inner stator inside radius (mm)	37.6
Inner stator outside radius(mm)	81.6
Axial length(mm)	80
Pole arc coefficients	1
Magnetization mode of permanent magnet	Radial magnetizing
Permanent magnet residual magnetization(T)	1.3
Relative permeability of permanent magnet	1.099
Thickness of PM (mm)	10
Thickness of modulation magnet pieces (mm)	13
Outer air-gap length(mm)	0.6
Inner air-gap length(mm)	0.6
Winding form	Single-layer chain
Number of parallel branches	1
Number of conductors per slot	55
Number of outer stator pole pairs	3
Number of modulation magnetic pieces	25
Number of inner stator slots	22

3. Optimization of the Motor Parameters

The working principle of flux modulation compound motor can be expressed as $n_s=P_1+P_2$, where the n_s is the number of modulating magnetic piece(mmp) of the magnetic ring , the P_1 is the number of pole pairs of outer stator windings and the P_2 is the number of inner permanent magnets. In this paper, $n_s=3$, p2 = 22, ns = 25. In order to obtain the maximum output torque of the motor, the magnetic flux density distribution, the back EMF waveform and the other factors were considered. The optimum design criterion of motor was determined and the quantitative analysis of the influence of motor performance index was made. Finally, the optimum scheme was determined. The optimization objectives include the proportion of magnetic blocks and the arc angle of the inner stator.

3.1 Optimization of the Proportion of Modulating Magnetic Pieces

As can be seen in Fig.3, one modulating magnetic piece and one nonmagnetic materials were defined as a group. The mechanical angle occupied by a group is defined as θ and the mechanical angle occupied by a modulation magnetic piece part is defined as θ_1.Hence, the proportion K can be defined as formula (4). The optimal proportional coefficient is determined by calculating and comparing the output torque and torque peak-to-peak of the motor at different proportions K.

$$K=\frac{\theta_1}{\theta} \tag{4}$$

The results obtained by the finite element analysis are shown in Fig. 4. During the calculation, the numbers of modulating magnetic piece and nonmagnetic materials in the magnetic ring are both 25. The stator winding is exerted with a sinusoidal current of 10A. According to the formula (4), the proportions K of the magnetic ring that range from 0.35 to 0.65. The maximum output torque and torque peak to peak are different with different proportions K. The output torque at 0.35 -0.45 is higher than other proportions but it becomes a downward trend after then. The peak-to-peak value of the torque is defined in formula (5). Apparently, it does not change significantly over the entire K-value range. As can be seen from the figure, the final selection of proportion K is 0.45.The the maximum output torque is 29.85Nm.

$$\frac{T_{max}-T_{min}}{T_{max}+T_{min}}\times 100\% \tag{5}$$

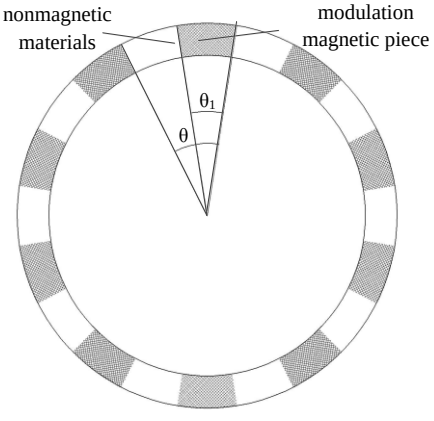

Fig.3. The proportion of modulation magnetic piece

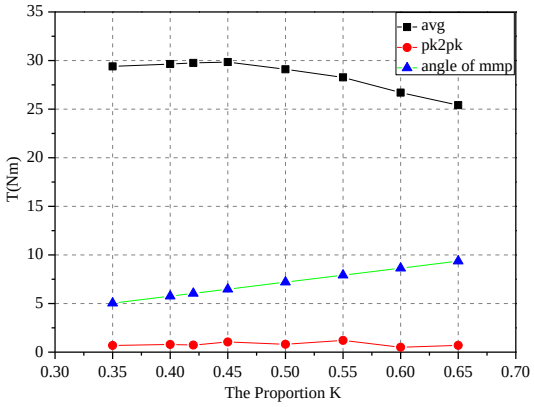

Fig. 4. The optimization result of Proportion K

3.2 Optimization of the Magnet Pole Arc Coefficient

The definition of the inner pole arc coefficient is shown in Fig.5, where the θ_1 is the optimization variable. During the optimization process, only change the value of θ_1 while the other parameters of the motor were not changed especially the cross-sectional area of the permanent magnet. The average output torque and torque peak and peak are shown in Fig.6.

It can be seen from the figure that the torque improves with the increase of the pole arc coefficient. The value of torque increase slowly after the pole arc coefficient is 9.5 and its peak to peak is acceptable. Considering the influence of saturation, the final determined angle of the inner stator pole of the motor is 9.5.

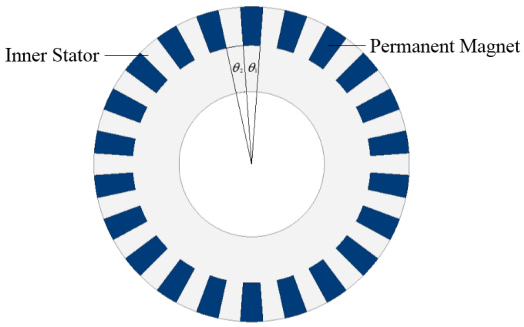

Fig. 5. The definition of arc angle inner stator

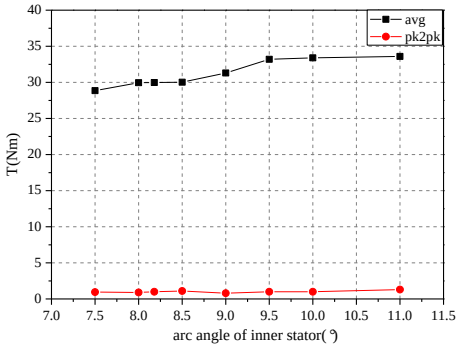

Fig. 6. The optimization result of arc angle

4. Comparison of Differnet Rotating Component

The optimized motor is established and the finite element method is carried to analysis the performance. The flux-modulation ring and the inner stator are taken as the rotor respectively, and the difference performance is compared. In the process of simulation, the rotor speed remains 600r / min.

4.1 Comparision of Air gap Flux Destiny

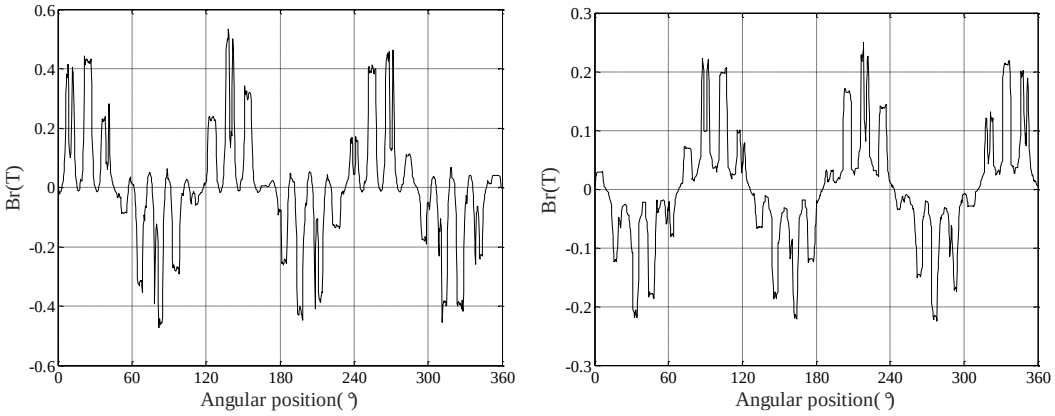

(a) (b)

Fig. 7. Radial flux destiny of outer air gap. (a: modulating ring rotor, b: inner rotor)

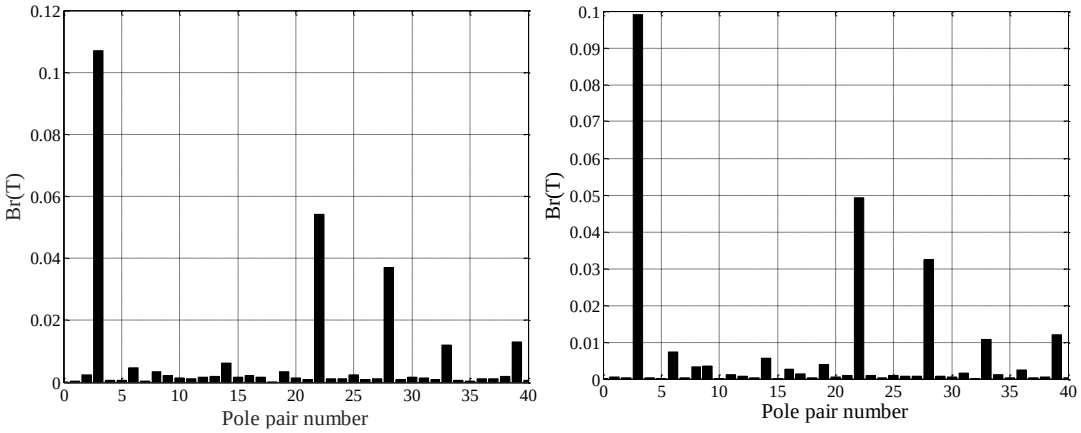

(a) (b)

Fig. 8. Harmonic analysis of the radial flux destiny. (a: modulating ring rotor, b: inner rotor)

The radial flux density of outer air gap is taken as the study object, the difference between the flux-modulation ring and the inner stator as rotor is compared. Figure 7 (a) and (b) are the flux destiny of the outer air-gap, and Figure 8 (a), (b) are the corresponding harmonic analysis. It can be seen that the flux density with flux-modulation ring rotor is bigger and the utilization of the PM is higher.

4.2 Comparision of Back-EMF

After the comparision of the flux destiny, Figure 9 (a) and (b) shows the the no-load back-EMF waveform respectively when the motor runs with differernt rotating component, that is, taking the flux-modulaiton ring as the rotor and the inner-stator as the rotor. Figure 10 (a) and (b) are the harmonic analysis of the no-load back-EMF, and it can be seen that the EMF is bigger if taking the flux-modulaiton ring as the rotor, but in the meanwhile, the total distorted rate of the harmonics gets smaller. It is found by contrast that the performances of the motor with modulating ring rotor are better than it with inner rotor, in section5, we mainly study the operating features of motor with modulating ring.

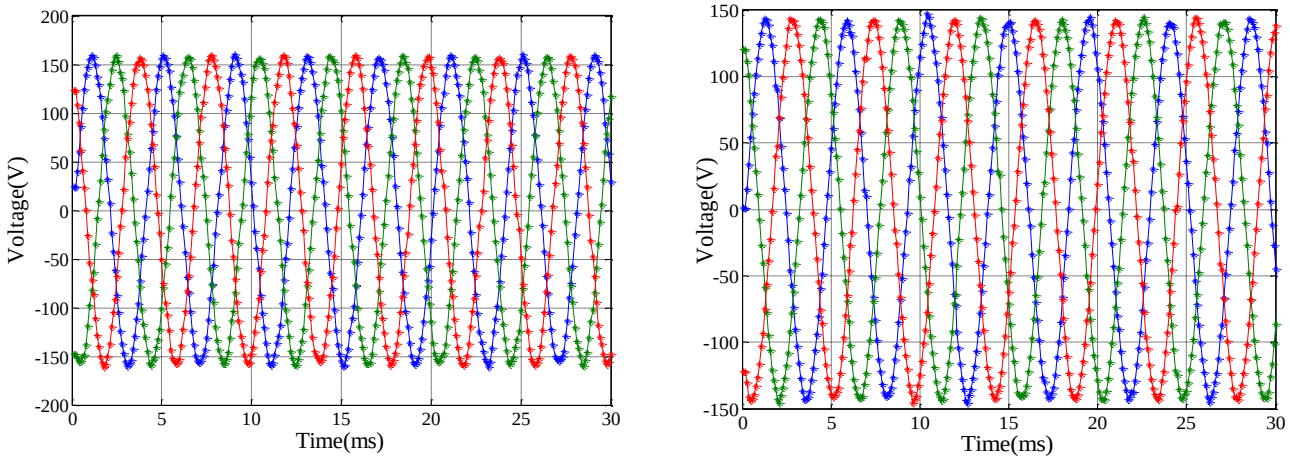

(a) (b)

Fig. 9. Back-EMF of no_load. (a: modulating ring rotor, b: inner rotor)

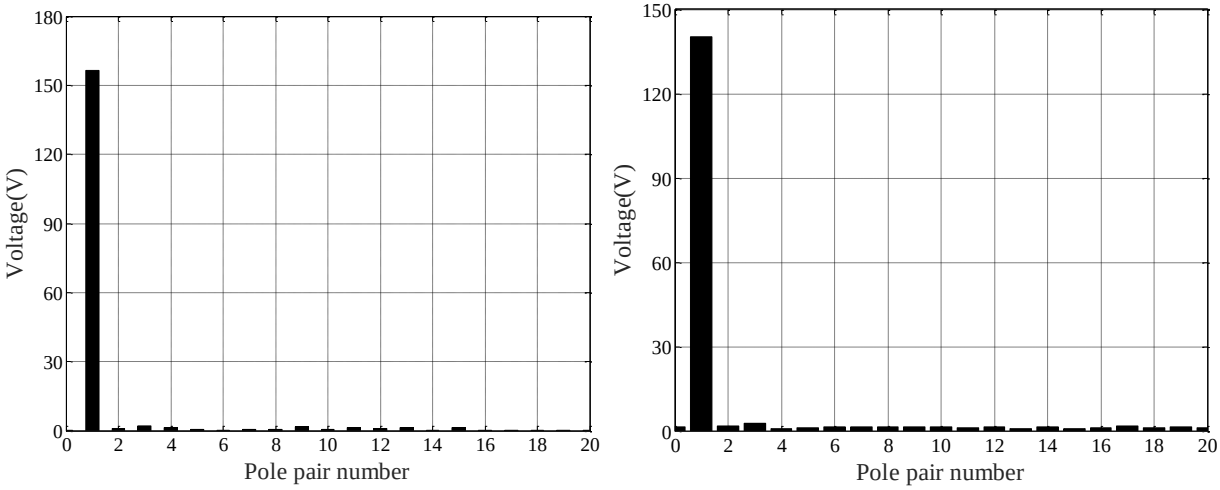

(a) (b)

Fig.10 . Harmonic analysis of the EMF (a: modulating ring rotor, b: inner rotor)

5. Performance of the Motor

5.1 Magnetic Field Distribution

The electromagnetic performance of the motor operating under no-load is analyzed, and the flux lines and flux destiny is showed in figure 11, including the mesh. It can be seen from the figure that the magnetic saturation is not very serious.

5.2 Torque of the Modulation Compound Motor

Figure12 shows the cogging torque of the motor and the output torque is showed in Figure 13, it can be seen that the cogging torque is small， meanwhile, the output torque is large and the ripple is low. The two figures indicate that the motor has the characteristics of low-speed large torque. Figure 14 shows the lock torque of the motor and it can be seen that it much more larger than the output torque, and we can concluded that the motor can bear greater load.

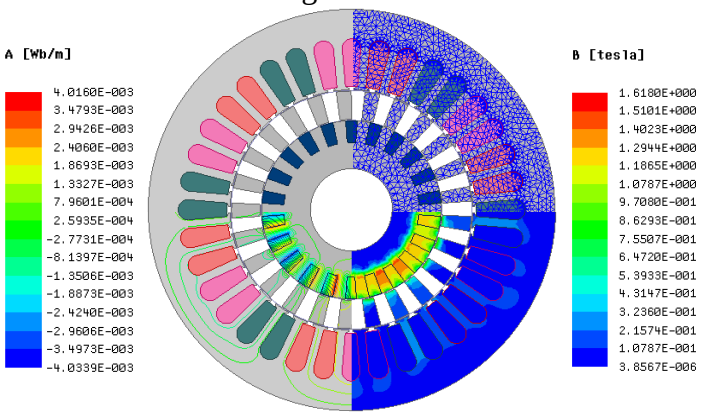

Fig.11. Magnetic field distribution of the motor.

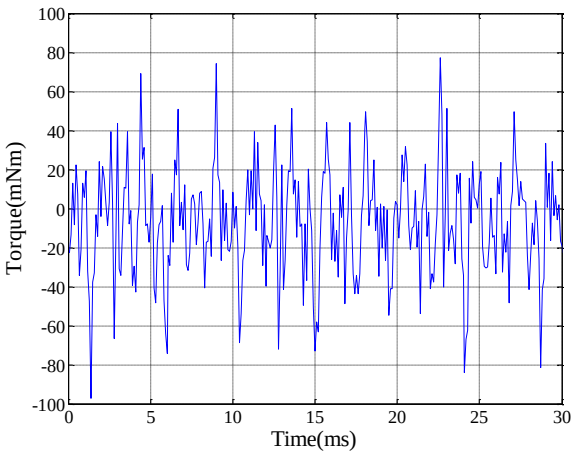

Fig. 12. Cogging torque of the motor.

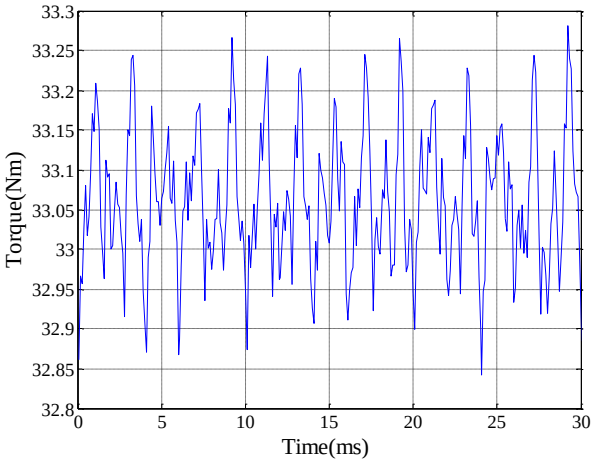

Fig. 13. Output torque of the motor.

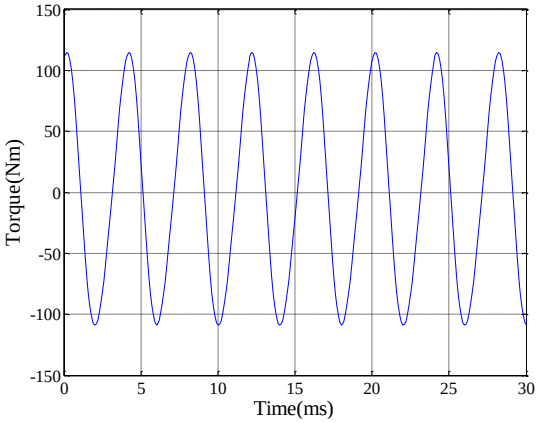

Fig. 14. Lock torque of the rotor

6. Conclusion

In this paper, a new class integrated magnetic-geared motor used in the oil pumping units, namely the IMGM, is proposed, which has the merits of the permanent magnet and magnetic gears. Hence, the proposed IMGM can provide the desired high-torque output for oil field system. The effect including the ratio K of the permeability section in the modulation ring and pole arc angle on the motor performance was researched specifically. The main influence of the torque characteristics and the prototype scheme of the Magnetic-Geared-Integrated machine was determined. The optimized motor both in the magnetic field distribution and its performance is superior to the basic design of the motor. In addition, by using the FEM, the static and dynamic performances of the machine is calculated. The machine characteristics and simulation results prove the validity of the machine design.

References

[1] K. Atallah, D. Howe, "A novel high performance magnetic gear," IEEE Trans on Magn, vol. 37, no. 4, 2001, pp. 2844–2846.

[2] K. Atallah, S. D. Calverley, and D. Howe, "Design, analysis and realisation of a high-performance magnetic gear," IEE Proc. Electr. Power Appl., vol. 151, no. 2, pp. 135–143, Mar. 2004.

[3] C.-C. Huang, M.-C. Tsai, D. G. Dorrell, and B.-J. Lin, "Development of a magnetic planetary gearbox," IEEE Trans. Magn., vol. 44, no. 3, pp. 403–412, Mar. 2008.

[4] Chunhua Liu, Jin Zhong, and K. T. Chau, "A Novel Flux-Controllable Vernier Permanent-Magnet Machine," IEEE Trans on Magn, vol. 47, no. 10, 2011, pp. 4238-4241.

[5] Jiangui Li, K. T. Chau, J. Z. Jiang, Chunhua Liu, and Wenlong Li, "A New Efficient Permanent-Magnet Vernier Machine for Wind Power Generation," IEEE Trans on Magn, vol. 46, no. 6, 2010, pp. 1475-1478.

[6] Yu Wang, Zhiquan Deng, and Xiaolin Wang, "A Parallel Hybrid Excitation Flux-SwitchingGenerator DC Power System Basedon Direct Torque Linear Control," IEEE Trans on Energy Conversion, vol. 27, no. 2, 2012, pp. 308-317.

[7] Ying Fan, Li Zhang, Ming Cheng, K. T. Chau, "Sensorless SVPWM-FADTC of a New Flux-Modulated Permanent-Magnet Wheel Motor Based on a Wide-Speed Sliding Mode Observer," IEEE Trans Ind. Elec, vol.62, no. 5, 2015, pp. 3143-3151.

[8] M.Aydin, S. Huang, and T. A. Lipo, "A newaxial flux surface mounted permanent magnet machine capable of field control," *Rec. Industry Applications Conf*., 37th IAS Annu. Meeting, vol. 2, 2002 pp.1250–1257.

[9] Ping Zheng, Jingang Bai, Chengde Tong, Jia Lin, Haipeng Wang, "Research on Electromagnetic Performance of a Novel Radial Magnetic-Field-Modulated Brushless Double-Rotor Machine," *Electrical Machine and Systems Conf.* (Hangzhou, China, August 20-23, 2011).